ONCOIMMUNOLOGY
2023, VOL. 12, NO. 1, 2207868
https://doi.org/10.1080/2162402X.2023.2207868

Taylor & Francis
Taylor & Francis Group

ORIGINAL RESEARCH

OPEN ACCESS Check for updates

Novel Fab-peptide-HLA-I fusion proteins for redirecting pre-existing anti-CMV T cell immunity to selective eliminate carcinoma cells

Isabel Britsch*, Anne P. van Wijngaarden*, Xiurong Ke, Mark. A.J.M. Hendriks, Douwe F. Samplonius, Emily M. Ploeg, and Wijnand Helfrich

Department of Surgery, Laboratory for Translational Surgical Oncology, University of Groningen, University Medical Center Groningen, Groningen, The Netherlands

ABSTRACT

Typically, anticancer CD8^{pos} T cells occur at low frequencies and become increasingly impaired in the tumor micro environment. In contrast, antiviral CD8^{pos} T cells display a much higher polyclonality, frequency, and functionality. In particular, cytomegalovirus (CMV) infection induces high numbers of 'inflationary' CD8^{pos} T cells that remain lifelong abundantly present in CMV-seropositive subjects. Importantly, these so-called inflationary anti-CMV T cells increase with age, maintain a ready-to-go state, populate tumors, and do not become exhausted or senescent. Given these favorable attributes, we devised a novel series of recombinant Fab-peptide-HLA-I fusion proteins and coined them 'ReTARGs'. A ReTARG fusion protein consists of a high-affinity Fab antibody fragment directed to carcinoma-associated cell surface antigen EpCAM (or EGFR), fused in tandem with soluble HLA-I molecule/β2-microglobulin, genetically equipped with an immunodominant peptide derived from CMV proteins pp65 (or IE-1). Decoration with EpCAM-ReTARG^{pp65} rendered EpCAM-expressing primary patient-derived carcinoma cells highly sensitive to selective elimination by cognate anti-CMV CD8^{pos} T cells. Importantly, this treatment did not induce excessive levels of proinflammatory T cell-secreted IFNγ. In contrast, analogous treatment with equimolar amounts of EpCAM/CD3-directed bispecific T-cell engager solitomab resulted in a massive release of IFNγ, a feature commonly associated with adverse cytokine-release syndrome. Combinatorial treatment with EpCAM-ReTARG^{pp65} and EGFR-ReTARG^{IE-1} strongly potentiated selective cancer cell elimination owing to the concerted action of the corresponding cognate anti-CMV CD8^{pos} T cell clones. In conclusion, ReTARG fusion proteins may be useful as an alternative or complementary form of targeted cancer immunotherapy for 'cold' solid cancers.

ARTICLE HISTORY
Received 22 February 2023
Revised 24 April 2023
Accepted 24 April 2023

KEYWORDS
Cancer immunotherapy; anti-CMV T cells; T cell-induced cytotoxicity; EpCAM; carcinoma

Introduction

Immunotherapeutic approaches based on PD-1/PD-L1-inhibitory antibodies are only effective in selected cancer types[1]. This may be related to the fact that most cancer types are considered to be immunologically 'cold' and fail to induce anticancer CD8^{pos} T cells due to defects in (neo)antigen presentation and absence of appropriate T cell activation signaling[2]. Consequently, potentially protective anticancer T cells occur at very low frequencies and become increasingly impaired in the tumor microenvironment due to cancer immunoediting[3].

In sharp contrast, CD8^{pos} T cells directed against persistent viruses such as cytomegalovirus (CMV) are maintained at high frequencies. Typically, symptomless CMV infection occurs at an early age, after which the virus latently persists in the body with occasional reactivation over time. Intriguingly, some of the induced anti-CMV T cell clones appear not to contract but rather increase with age, a phenomenon known as T cell inflation[4]. Of note, in healthy CMV-seropositive elderly individuals, up to 20% of the entire CD8^{pos} T cell repertoire may be directed against immunodominant peptides derived from CMV proteins[5]. In particular, inflationary anti-CMV CD8^{pos} T cells are predominantly directed toward selected immunodominant peptides derived from CMV proteins pp65, IE-1, and IE-2[6,7]. Inflationary anti-CMV CD8^{pos} T cells have an effector-memory phenotype, are PD-1^{low}, and maintain a *ready-to-go* functional status that does not require additional co-stimulatory signals[8–10]. Moreover, inflationary anti-CMV CD8^{pos} T cells do not adopt a typical tissue-resident memory phenotype but retain full capacity to migrate into virtually all tissues. Remarkably, recent data indicate that CMV-specific T cells extend their surveillance to malignant tissues and populate human tumors as functional competent 'bystander-CTLs'[11,12]. Thus, unlike anticancer CD8^{pos} T cells, homing of anti-CMV CD8^{pos} T cells to the tumor bed does not seem to be hampered.

These unique features have led to the development of strategies to redirect anti-CMV CD8^{pos} T cells to eliminate cancer cells. In particular, this involved the construction of recombinant fusion proteins consisting of the CMV pp65-derived CTL

CONTACT Wijnand Helfrich w.helfrich@umcg.nl Department of Surgery, Laboratory for Translational Surgical Oncology, University Medical Center Groningen, Hanzeplein 1, Groningen 9713 GZ, The Netherlands

*Contributed equally.

Supplemental data for this article can be accessed online at https://doi.org/10.1080/2162402X.2023.2207868.

epitope NLVPMVATV (NLV), soluble HLA-A × 02:01, and a tumor-directed antibody or fragment thereof. Schmittnaegel *et al.* (2015,2016) described an extensive series of NLV/HLA-A × 02:01 based fusion proteins directed against insulin-like growth factor 1 receptor (IGF1R) or melanoma-associated chondroitin sulfate proteoglycan (MCSP)[13,14].

However, individuals with both HLA-A × 02:01 and HLA-B × 07:02 alleles show dominance in terms of anti-CMV_{pp65} $CD8^{pos}$ T cell numbers specific for peptide TPRVTGGGAM (TPR)[5]. Additionally, HLA-B × 07:02-restricted TPR-specific $CD8^{pos}$ T cells preferentially expanded compared to HLA-A × 02:01-restricted NLV-specific $CD8^{pos}$ T cells[15]. Moreover, CMV-seropositive subjects heterozygous for the HLA-B × 07:02 allele harbored a larger percentage of $CD8^{pos}$ tetramer-reactive T cells than donors who were heterozygous for HLA-A × 02:01[16].

These observations prompted us to develop a monomeric single-chained recombinant fusion protein, designated epithelial cell adhesion molecule (EpCAM)-$ReTARG^{pp65}$, in which the CMV pp65 peptide TPR, soluble HLA-B × 07:02/β2-microglobulin (β2 M) molecule, and EpCAM-directed Fab domain were genetically fused in tandem. We selected EpCAM as the target antigen because it is overexpressed in a broad variety of human carcinomas[17]. Importantly, EpCAM expression in nonmalignant tissue is low and mostly limited to the basolateral surface of the epithelia.

Additionally, it was demonstrated that HLA-C × 07:02-restricted anti-CMV $CD8^{pos}$ T cells directed at the IE-1-derived peptide CRVLCCYVL expanded enormously during healthy aging without signs of exhaustion[18]. Hence, we constructed and evaluated the fusion protein epidermal growth factor receptor (EGFR)-$ReTARG^{IE\text{-}1}$ with the engineered capacity to redirect HLA-C × 07:02-restricted anti-$CMV_{IE\text{-}1}$ $CD8^{pos}$ T cells to attack cancer cells in an EGFR-directed manner.

Here, we demonstrate the potent capacity of EpCAM-$ReTARG^{pp65}$ to selectively redirect the cytotoxic potential of HLA-B × 07:02-restricted TPR-specific anti-CMV $CD8^{pos}$ T cells toward various EpCAM-expressing cancer cell lines and primary patient-derived carcinoma cells. Importantly, during EpCAM-$ReTARG^{pp65}$-mediated elimination of cancer cells, T cell-secreted cytokine levels did not appear to be excessively elevated. In contrast, analogous treatment with equimolar amounts of the EpCAM/CD3-directed bispecific T cell engager solitomab resulted in excessive release of IFNγ, a feature commonly associated with cytokine-release syndrome. Combinatorial treatment of carcinoma cells with EpCAM-$ReTARG^{pp65}$ and EGFR-$ReTARG^{IE\text{-}1}$ strongly potentiated cancer cell elimination, likely due to the concurrent cytolytic action of the respective cognate anti-CMV $CD8^{pos}$ T cell clones. Importantly, during combinatorial treatment, T cell-secreted cytokine levels were only slightly elevated compared to single-agent treatment.

Taken together, our results suggest that EpCAM-$ReTARG^{pp65}$ and EGFR-$ReTARG^{IE\text{-}1}$ show promising capacity to redirect highly prevalent antiviral T cell clones to selectively eliminate cancer cells while mitigating the risk of immune-related side effects associated with conventional T cell recruiters. Our ReTARG approach may be useful as a complementary and/or alternative treatment for cancer immunotherapy.

Materials and methods

Antibodies and reagents

The following primary fluorescently labeled monoclonal antibodies directed against human antigens were used: FITC-labeled anti-EpCAM antibody (STEMCELL Technologies, clone VU-1D9), APC-labeled anti-HLA-B7 (clone BB7.1, BioLegend), APC-labeled anti-β2-microglobulin (clone 2 M2, BioLegend), PerCP-Cy5.5-labeled anti-CD3 (clone OKT-3, eBioscience), PE-labeled anti-CD3 antibody (Immunotools), APC-labeled anti-CD8 (clone RPA-T8, eBioscience), FITC-labeled anti-CD8 antibody (Immunotools), PE-labeled anti-CD137 (clone 4B4–1, BD Pharmingen), PerCP-eFluor710-labeled anti-CCR7 (clone 3D12, eBioScience), FITC-labeled anti-CD45RA (Immunotools), FITC-labeled anti-CD69 (Immunotools), APC-labeled anti-CD107a (clone H4A3, BD Bioscience), APC-labeled anti-CD25 (Immunotools), PerCP-Cy5.5-labeled anti-CD28 (clone CD28.2, eBioscience), PE-labeled anti-PD-1 (clone MIH4, eBioscience), APC-labeled anti-TIM-3 (clone F38-2E2, eBioscience) and PE-labeled anti-LAG-3 (R&D Systems). The following reagents were used: FITC-labeled Annexin-V (Immunotools), APC-labeled MHC-I dextramer HLA-B × 07:02/TPRVTGGGAM (TPR-dextramer, Immudex), propidium iodide (PI) (Invitrogen), Vybrant DiD (Thermo Fisher), cell-permeable fluorescent dye CFSE CellTrace Far Red (Thermo Fisher) and Brefeldin A Solution (eBioscience). Solitomab (AMG 110, formerly known as MT110), a bispecific EpCAM/CD3 T cell engager, was obtained from ProteoGenix. The following ELISAs were used: Granzyme B (Mabtech) and IFNγ (eBioscience).

Cell lines and transfectants

Cell lines A375M, A-431, FaDu, NCI-H292, OvCAR-3, HEK293T, MDA-MB-231, SK-N-SH, PC-3 M, Sk-Br-3, NCI-H322, MCF-7, DLD-1, PANC-1, and Ca Ski were obtained from the ATCC (Manassas, VA). The cells were cultured in RPMI-1640 or DMEM (Lonza) supplemented with 10% FCS at 37°C in a humidified 5% CO_2 atmosphere. Cells stably expressing CMV pp65 protein were generated by lipofection (Fugene-HD, Promega) of the plasmid pCMV6-pp65 (Origene). Ectopic expression of the CMV protein pp65 in transduced cell lines was evaluated after 48 h by immunocytochemistry using an anti-CMV pp65 antibody cocktail (IQ Products) and HRP-conjugated rabbit anti-mouse antibody (Dako). Cell lines OvCAR-3.TM-$ReTARG^{pp65}$ and A375M.TM-$ReTARG^{pp65}$ expressing transmembrane pp65-HLA-B × 07:02 were produced by transfection with the plasmid pcDNA3.1-hygro-pp65-B7-TM. Cells stably expressing human EpCAM-YFP were generated by lipofection of the plasmid pEpCAM-YFP-N1. Clones with stable expression of the indicated transgenes were selected using culture medium supplemented with the appropriate antibiotic. EpCAM surface expression was evaluated by flow cytometry using an anti-EpCAM antibody. For flow cytometric analyses, Guava easyCyte

6-2 L Benchtop Flow Cytometer and Guava InCyte 3.2 software were used. PC-3 M.EpCAM-KO cells were generated using CRISPR-Cas9 gene-editing technology by transfection with plasmid pSpCas9 BB-2A-GFP (PX458) containing the EpCAM-targeting sgRNA 5′-TAATGTTATCACTATTGATC-3'[19] followed by single-cell sorting.

Primary patient-derived malignant cells

Tissues from patients with stage IIIC high-grade serous ovarian cancer were collected during primary cytoreductive surgery. The use of anonymous rest materials is regulated by the code for good clinical practice in the Netherlands. The requirement for informed consent was waived in accordance with Dutch regulations. Excised tumor tissue was incubated in pre-warmed collagenase A (Roche) solution and then homogenized using a gentleMACS Dissociator (Miltenyi Biotec). Subsequently, cancer cells were cultured in RPMI-1640 supplemented with 10% FCS serum at 37°C in a humidified 5% CO_2 atmosphere.

Generation and ex vivo expansion of anti-CMV_{pp65} and anti-$CMV_{IE\text{-}1}$ $CD8^{pos}$ T cells

After obtaining informed consent, peripheral blood mononuclear cells (PBMCs) were isolated from heparinized blood from one CMV-seronegative/HLA-B × 07:02^{pos} and four CMV-seropositive/HLA-B × 07:02^{pos}/HLA-C × 07:02^{pos} healthy volunteers using standard density gradient centrifugation (Lymphoprep, Stemcell Technologies). PBMCs were harvested, washed, and cultured in 6-well plates (5×10^6/ml) in X-VIVO15 medium (Lonza). PBMCs were stimulated with either recombinant CMV pp65 (Miltenyi Biotech) or T cell-activated IE-1 (Lophius Biosciences) protein solution for 2 d. Next, stimulated PBMCs were harvested, resuspended in fresh X-VIVO15 medium supplemented with 500 U/ml IL-2 (Immunotools), and cultured for an additional 4 d. Subsequently, CMV_{pp65}- and $CMV_{IE\text{-}1}$-stimulated PBMCs were cultured on a feeder layer of OvCAR-3.pp65 cells and OvCAR-3.IE-1 at an effector-to-target (E:T) cell ratio of 7.5:1. Restimulated T cells were harvested, washed, resuspended in X-VIVO15 medium supplemented with 500 U/ml IL-2, and cultured for 6 d. The latter two expansion steps were repeated once a week. Expanded anti-CMV $CD8^{pos}$ T cells were cultured and utilized until stimulation round eight. Flow cytometry indicated that this stimulation protocol yielded up to 60% TPR-dextramer^{pos} $CD8^{pos}$ T cells.

Construction of ReTARGs

EpCAM-ReTARG^{pp65} was designed as a monomeric single-chained recombinant fusion protein consisting of the antigenic CMV pp65 peptide TPRVTGGGAM (TPR), β2-microglobulin, and a truncated HLA-B × 07:02 heavy chain lacking transmembrane and intracellular domains. To enhance the stability of EpCAM-ReTARG^{pp65}, TPRVTGGGAM was C-terminally fused to the linker sequence GCGGSGGGGSGGGGS, which was engineered to contain a cysteine residue (in bold), which allowed the formation of an intramolecular disulfide bridge with a cysteine residue inserted in the α1 domain HLA-B × 07:02 heavy chain. Using a flexible linker, the HLA-I-α chain was genetically fused to an anti-EpCAM Fab antibody domain containing VH-VL gene segments of the humanized antibody fragment scFv 4D5 MOC-B[20]. An analogous ReTARG variant with irrelevant target specificity, designated Mock-ReTARG^{pp65}, was constructed by exchanging the anti-EpCAM Fab for an anti-CD19 Fab domain containing VH-VL gene segments from tafasitamab (MOR208). Similarly, EGFR-ReTARG$^{IE\text{-}1}$ was constructed as a monomeric single-chained protein consisting of the immunodominant CMV IE-1-derived peptide CRVLCCYVL (CRV), β2 M, and a truncated HLA-C × 07:02 heavy chain lacking transmembrane and intracellular domains. Using a flexible linker, the HLA-I-α chain was genetically fused to an anti-EGFR Fab antibody domain containing VH-VL gene segments of mAb 425[21].

Production and purification of ReTARGs

EpCAM-ReTARG^{pp65}, EGFR-ReTARG$^{IE\text{-}1}$, and Mock-ReTARG^{pp65} were produced after lipofection (Fugene-HD, Promega) of the corresponding encoding plasmids into HEK293T cells. After 7 d, conditioned cell culture supernatants were harvested and cleared by centrifugation (3000 × g, 30 min). ReTARGs were purified using a Capture Select^{TM} CH1-XL column (Thermo Fisher) connected to an ÄKTA Start chromatography system (GE Healthcare Life Sciences), diluted in PBS to 1 mg/ml, and stored at −20°C until use.

SDS-PAGE analysis

Purified EpCAM-ReTARG^{pp65} (2 µg/lane) under reducing or non-reducing conditions were separated by SDS-PAGE (10% acrylamide) and stained using Coomassie brilliant blue.

Assessment of target antigen-selective binding activity

The binding of EpCAM-ReTARG^{pp65}, EGFR-ReTARG$^{IE\text{-}1}$, and Mock-ReTARG^{pp65} toward cell surface-expressed EpCAM or EGFR was assessed by flow cytometry. In short, EpCAM^{pos} or EGFR^{pos} cancer cells were incubated with increasing amounts (1–10,000 ng/ml) of the indicated ReTARG at 4°C for 45 min, after which binding was evaluated using either anti-HLA-B7 or anti-β2 M antibody.

In vitro cytotoxicity assays

Freshly isolated PBMCs (from CMV-seropositive/HLA-B × 07:02^{pos}/HLA-C × 07:02^{pos} healthy volunteers) were cultured overnight in medium supplemented with 50 U/ml IL-2 and then co-cultured with OvCAR-3.pp65 or PC-3 M cancer cells at the indicated E:T cell ratios in the presence (or absence) of EpCAM-ReTARG^{pp65} or/and EGFR-ReTARG$^{IE\text{-}1}$ for 4 d. Subsequently, induction of apoptotic cancer cell death was evaluated by LDH release (CytoTox 96 Non-Radioactive Cytotoxicity Assay, Promega) and Annexin V/PI staining using flow cytometry. *Ex vivo*-expanded anti-CMV_{pp65} $CD8^{pos}$ and/or anti-$CMV_{IE\text{-}1}$ $CD8^{pos}$ T cells were co-cultured for 24 h with a series of cancer cell lines and primary patient-derived ovarian cancer cells, in the presence (or absence) of

EpCAM-ReTARG^{pp65}, EGFR-ReTARG^{IE-1}, Mock-ReTARG^{pp65}, and solitomab, respectively, at the indicated E:T cell ratios. Subsequently, apoptotic cancer cell death was evaluated by flow cytometry (Annexin V/PI staining), LDH release, real-time cell analysis (xCELLigence), and live cell imaging (IncuCyte S3) using NucView 488 Caspase-3/8 Substrate (Biotium).

pH and temperature stability

Assessment of thermostability: EpCAM-ReTARG^{pp65} was stored in PBS at −20, 4, and 37°C for 3 d. Assessment of pH stability: EpCAM-ReTARG^{pp65} was stored in 20 mM acetate buffer, at pH 4.0, 5.0, 6.0, or 7.0 at 4°C for 3 d. Subsequently, remaining capacities of EpCAM-ReTARG^{pp65} to bind to EpCAM^{pos} target cells and to redirect the cytotoxic activity of anti-CMV$_{pp65}$ CD8^{pos} T cells toward EpCAM^{pos} PC-3 M cancer cells were evaluated essentially as described above.

T cell activation assays

The activation of anti-CMV$_{pp65}$ CD8^{pos} T cells in response to treatment with EpCAM-ReTARG^{pp65} was determined by evaluating T cell aggregate formation. *Ex vivo*-expanded CFSE-labeled anti-CMV$_{pp65}$ CD8^{pos} T cells were co-cultured (or not) with PC-3 M cells in the presence of EpCAM-ReTARG^{pp65} and Mock-ReTARG^{pp65}. Clustering of T cells (red area) was evaluated using live cell imaging. Alternatively, the activation status of PBMCs, anti-CMV$_{pp65}$ CD8^{pos}, and anti-CMV$_{IE-1}$ CD8^{pos} T cells was assessed by flow cytometric analysis of CD137 exposure on CD3^{pos}/CD8^{pos} T cells and by measuring Granzyme B and IFNγ excretion using the corresponding ELISAs.

Statistical analysis

Statistical analyses were performed using GraphPad Prism 8 (GraphPad Software). All *in vitro* cytotoxicity assays evaluated by flow cytometry (Annexin V/PI staining) represent mean ± SD of three independent experiments (with two technical replicates, respectively), unless indicated otherwise. All other assays were conducted in three independent experiments (with two technical replicates, respectively), but show representative graphs with mean ± SD of one experiment, unless indicated otherwise. Means were assessed for differences using an unpaired two-tailed Student's t-test and one- or two-way ANOVA, respectively, followed by a multiple comparisons test, where appropriate. *P*-values considered significant are indicated by asterisks as follows: $^{*}p < .05$; $^{**}p < .01$; $^{***}p < .001$; $^{****}p < .0001$.

Results

EpCAM-ReTARG^{pp65} selectively and dose-dependently binds to EpCAM^{pos} cancer cells

We successfully constructed the fusion protein EpCAM-ReTARG^{pp65} in which the CMV pp65 peptide TPR, soluble HLA-B × 07:02/β2 M molecule, and an EpCAM-directed Fab domain were fused in tandem (Figure 1a; mode of action: Figure 1b). To characterize its binding properties, EpCAM-ReTARG^{pp65} was purified to near homogeneity. Under non-reducing conditions, EpCAM-ReTARG^{pp65} migrated as a single protein band with an apparent molecular weight of ~ 100 kDa (Figure 1c, lane 1). This is in good agreement with the calculated molecular weight (MW) of 97,387.8 Da. Under reducing conditions, EpCAM-ReTARG^{pp65} migrated as two protein bands of ~ 70 kDa (calculated MW = 73,365.4 Da) and~24 kDa (calculated MW = 24,040.9 Da) (Figure 1c, lane 2). The 24 kDa protein band represents the light chain of the EpCAM-targeting Fab domain. EpCAM-ReTARG^{pp65} showed selective and dose-dependent binding capacity toward EpCAM-expressing PC-3 M cancer cells, whereas Mock-ReTARG^{pp65}, an analogous fusion protein with irrelevant targeting specificity, failed to do so (Figure 1d). Moreover, EpCAM-ReTARG^{pp65} did not bind PC-3 M.EpCAM-KO cells (Figure 1e). Similarly, EpCAM-ReTARG^{pp65} selectively bound to A375M.EpCAM melanoma cells but not to parental EpCAM^{neg} A375M cells (Figure 1f).

Frequency of anti-CMV$_{pp65}$ CD8^{pos} T cells in freshly isolated PBMCs from CMV-seropositive/HLA-B × 07:02^{pos} donors is sufficient to potently eliminate CMV pp65-expressing cancer cells

PBMCs freshly isolated from CMV-seropositive/HLA-B × 07:02^{pos} donors #1 to #4 or CMV-seronegative/HLA-B × 07:02^{pos} donor #5 were evaluated for their respective maximal capacities to selectively eliminate HLA-B × 07:02-matched OvCAR-3. pp65 cancer cells (Figure 2a). PBMCs derived from CMV-seropositive donors contained sufficient *ready-to-go* anti-CMV$_{pp65}$ CD8^{pos} T-cells and selectively eliminated OvCAR-3. pp65 cancer cells at a 20:1 E:T cell ratio without the need for expansion or additional stimuli. Next, PBMCs from donors #1 to #5 were assessed for their respective percentages of TPR-dextramer^{pos} anti-CMV$_{pp65}$ CD8^{pos} T cells, which ranged from 0.62% to 3.88%. PBMCs from CMV-seronegative/HLA-B × 07:02^{pos} donor #5 did not contain TPR-selective anti-CMV$_{pp65}$ CD8^{pos} T cells. A 15 day *ex vivo*-expansion yielded up to~60% TPR-dextramer^{pos} anti-CMV$_{pp65}$ CD8^{pos} T cells (Figure 2b). Of note, *ex vivo*-expanded anti-CMV$_{pp65}$ CD8^{pos} T cells mainly exhibited an effector memory phenotype (Figure S1).

Ex vivo-expanded anti-CMV$_{pp65}$ CD8^{pos} T cells potently eliminate CMV pp65-expressing cancer cells at low E:T cell ratios

Ex vivo-expanded anti-CMV$_{pp65}$ CD8^{pos} T cells from all four CMV-seropositive donors eliminated OvCAR-3. pp65 cells, whereas the T cells of donor #5 failed to do so (Figure 2c). Compared with unstimulated PBMCs, *ex vivo*-expanded HLA-B × 07:02-restricted anti-CMV$_{pp65}$ CD8^{pos} T cells eliminated OvCAR-3. pp65 cancer cells to similar levels at a 10× lower E:T cell ratio (2:1). Moreover, the addition of anti-CMV$_{pp65}$ CD8^{pos} T cells from donors #1 to #4 to OvCAR-3. pp65 cancer cells potently enhanced the exposure of CD137 on the effector T cells, indicating their antigen-specific activation (Figure 2d).

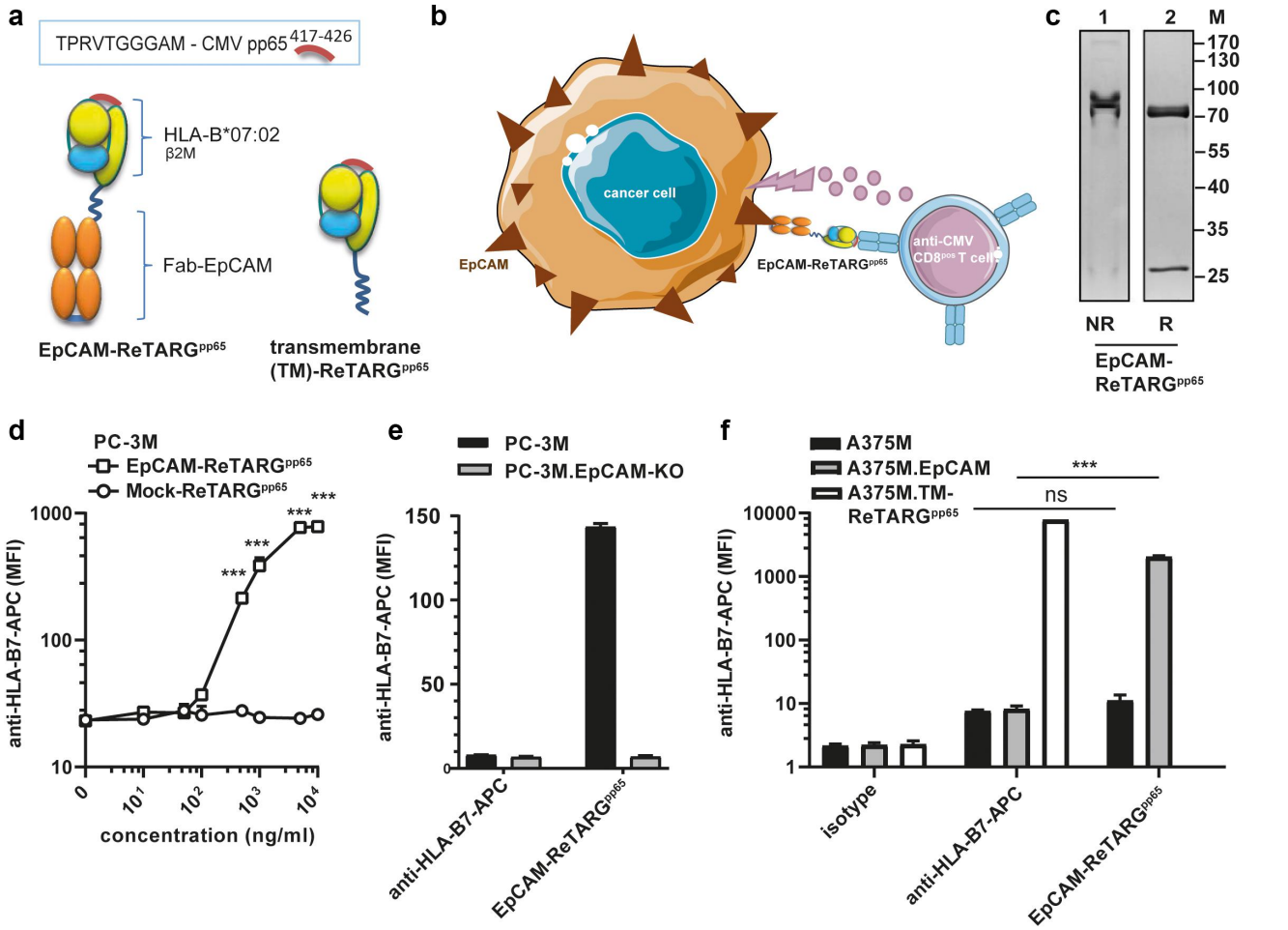

Figure 1. EpCAM-ReTARG^{pp65} selectively and dose-dependently binds to EpCAM^{pos} cancer cells. (a) Schematic representation of transmembrane(TM)-ReTARG^{pp65} and EpCAM-ReTARG^{pp65} fusion proteins. The anti-EpCAM Fab domain of EpCAM-ReTARG^{pp65} was constructed using published VH and VL gene sequences of the humanized antibody fragment scFv 4D5 MOC-B[20]. (b) Proposed mode-of-action of EpCAM-ReTARG^{pp65}. EpCAM-ReTARG^{pp65} binds via its anti-EpCAM Fab antibody domain to cell surface-exposed EpCAM on cancer cells. TPR peptide-equipped HLA-B × 07:02/β2 M recruits cognate anti-CMV$_{pp65}$ CD8^{pos} T cells, which mediate cancer cell death by releasing apoptosis-inducing agents, such as granzymes and perforins. (c) SDS-PAGE analysis with Coomassie brilliant blue staining of EpCAM-ReTARG^{pp65} under non-reducing (NR, lane 1) and reducing (R, lane 2) conditions. *M* = marker. (d) Concentration-dependent binding of EpCAM-ReTARG^{pp65} and Mock-ReTARG^{pp65} to EpCAM^{pos} PC-3 M cancer cells. (e) Binding of EpCAM-ReTARG^{pp65} (0.5 µg/ml) to EpCAM^{pos} PC-3 M vs PC-3 M.EpCAM-KO cancer cells. (f) Binding of EpCAM-ReTARG^{pp65} (1 µg/ml) to EpCAM^{neg} A375M and A375 M.EpCAM melanoma cells. A375M.TM-ReTARG^{pp65} cells were used as a positive control. Graphs in D-F were assessed by flow cytometry and representative images with two technical replicates are shown (mean ± SD). *n* = 3. Statistical analysis in D was performed using two-way ANOVA followed by Bonferroni-Dunn post-hoc test. Statistical analysis in F was performed using unpaired t-test (anti-HLA-B7-APC vs EpCAM-ReTARG^{pp65} per cell line). (ns = not significant, ***p < .001).

In line with this, enhanced exposure of additional activation and co-stimulatory markers was also observed, whereas exposure of co-inhibitory markers remained low (Figure S1). Notably, the HLA-B × 07:02-matched OvCAR-3. pp65 cells were eliminated by HLA-B × 07:02-restricted anti-CMV$_{pp65}$ CD8^{pos} T cells, whereas HLA-B × 07:02^{neg} FaDu.pp65 cells were unaffected (Figure 2e). Apoptotic cancer cell death was evaluated by flow cytometry, LDH release, real-time cell analysis, or live cell imaging. All of these measurement techniques lead to equivalent results and can be used interchangeably (Figure S2).

EpCAM-ReTARG^{pp65} engages anti-CMV$_{pp65}$ CD8^{pos} T cells in an EpCAM-selective manner

The capacity of EpCAM-ReTARG^{pp65} to selectively mediate cancer cell elimination was investigated. Coculture of *ex vivo*-expanded anti-CMV$_{pp65}$ CD8^{pos} T cells with parental A375M cancer cells in the presence of EpCAM-ReTARG^{pp65} did not result in cancer cell elimination (Figure 3a), whereas identically treated A375M.EpCAM cancer cells were efficiently eliminated (Figure 3b). Anti-CMV$_{pp65}$ CD8^{pos} T cells also lysed A375M. transmembrane(TM)-ReTARG^{pp65} cancer cells in the absence of EpCAM-ReTARG^{pp65} (Figure 3c). The elimination capacities of A375M.EpCAM cells in the presence of EpCAM-ReTARG^{pp65} and A375M.TM-ReTARG^{pp65} cells in the absence of EpCAM-ReTARG^{pp65} were equivalent. Moreover, EpCAM-ReTARG^{pp65} was able to redirect the cytotoxic activity of *ex vivo*-expanded anti-CMV$_{pp65}$ CD8^{pos} T cells toward EpCAM^{pos} parental PC-3 M cancer cells, whereas PC-3 M. EpCAM-KO cells remained unaffected (Figure 3d,e-f).

EpCAM-ReTARG^{pp65} selectively activates cytotoxic effector potential of anti-CMV$_{pp65}$ CD8^{pos} T cells

Next, we assessed whether EpCAM-ReTARG^{pp65} selectively activates the cytotoxic potential of anti-CMV$_{pp65}$ CD8^{pos} effector T cells. To this end, *ex vivo*-expanded

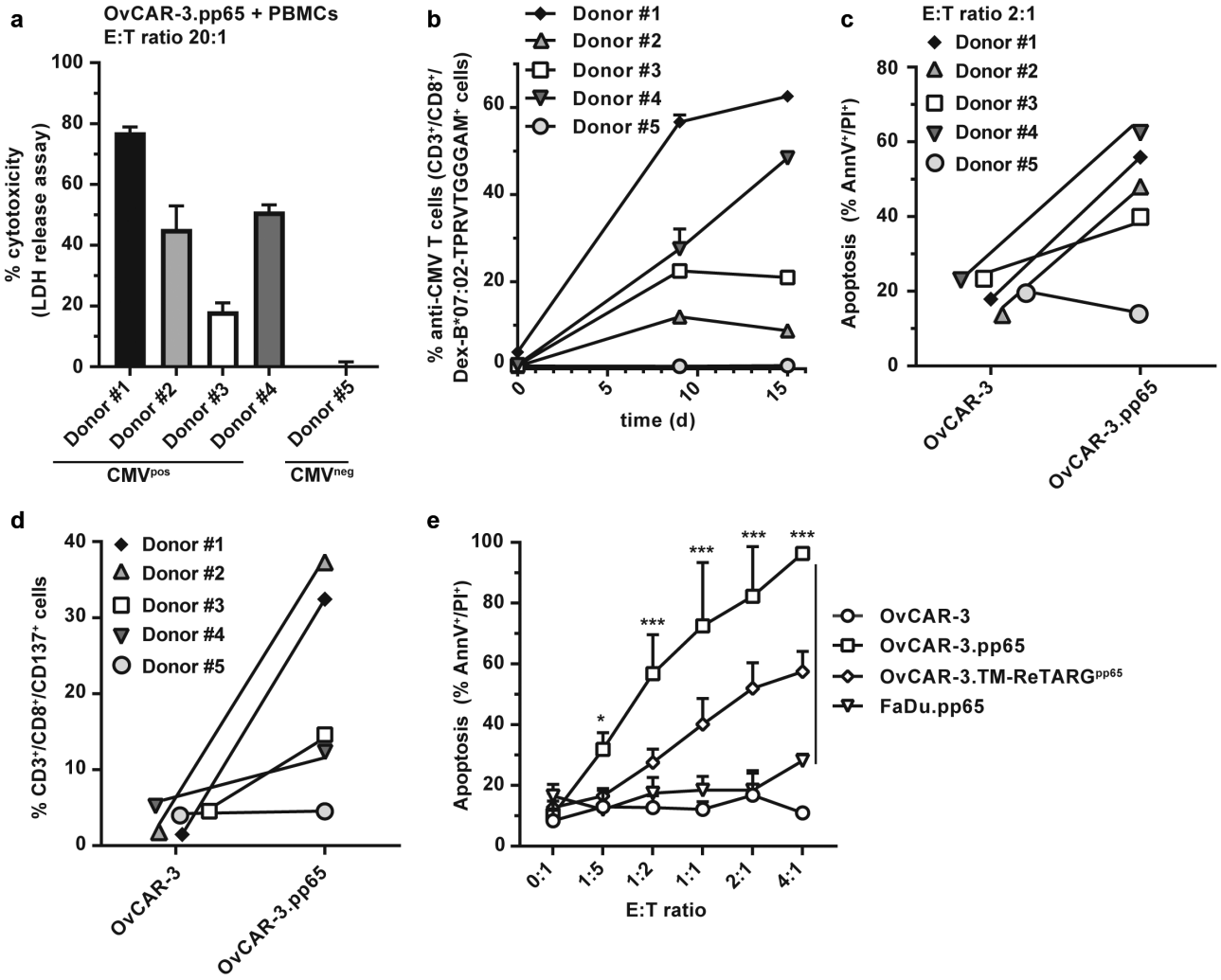

Figure 2. Ex vivo-expanded anti-CMV_{pp65} $CD8^{pos}$ T cells potently eliminate CMV pp65-expressing cancer cells at low E:T cell ratios (a) Cytotoxic capacity of PBMCs isolated freshly from 4 CMV-seropositive/HLA-B × 07:02^{pos} donors and 1 CMV-seronegative/HLA-B × 07:02^{pos} donor toward OvCAR-3.Pp65 cancer cells (E:T cell ratio = 20:1). Elimination of OvCAR-3.Pp65 cancer cells was evaluated after 4 d using a standard LDH release cytotoxicity assay. (b) Percentage of anti-CMV_{pp65} $CD8^{pos}$ T cells per donor was evaluated by staining for TPR-dextramer^{pos} T cells. (c) Cytotoxic capacity of stimulated and expanded anti-CMV_{pp65} $CD8^{pos}$ T cells toward OvCAR-3.Pp65 cells (E:T cell ratio = 2:1). Apoptotic cancer cell death was assessed using Annexin-V/PI staining after 24 h. (d) Antigen-specific activation status (CD137 exposure) of anti-CMV_{pp65} $CD8^{pos}$ T cells as used in C. (e) Cytotoxic capacity of stimulated and expanded anti-CMV_{pp65} $CD8^{pos}$ T cells toward OvCAR-3, OvCAR-3.Pp65 (Hla-b × 07:02-matched) and FaDu.Pp65 (Hla-b × 07:02-unmatched) cancer cells at increasing E:T cell ratios. Apoptotic cancer cell death was assessed using Annexin-V/PI staining after 24 h. OvCAR-3.transmembrane(TM)-ReTARG^{pp65} cells were used as a positive control. Graphs a and B show representative images with two technical replicates (mean ± SD). Graphs C and D: $n = 1$ (two technical replicates). Graph E: $n = 3$ (two technical replicates), mean ± SD are shown and statistical analysis was performed using two-way ANOVA followed by Bonferroni-Dunn post-hoc test (OvCAR-3.Pp65 vs. FaDu.Pp65 cells). (*p < .05, ***p < .001).

anti-CMV_{pp65} $CD8^{pos}$ T cells were cocultured (or not) with $EpCAM^{pos}$ cancer cells in the presence of EpCAM-ReTARG^{pp65} or Mock-ReTARG^{pp65}. Indeed, enhanced CD137 exposure, increased excretion of Granzyme B and IFNγ, and T cell aggregate formation (both number and size) were observed only in the combined presence of $EpCAM^{pos}$ PC-3 M target cells and EpCAM-ReTARG^{pp65} (Figure 4a,b,c). Treatment with EpCAM-ReTARG^{pp65} enhanced T cell-secreted IFNγ in the presence of PC-3 M target cells in a dose-dependent manner, whereas Mock-ReTARG^{pp65} failed to do so under the same conditions (Figure 4d). Analogously, EpCAM-ReTARG^{pp65} did not enhance T cell-secreted IFN-γ in the presence of PC-3 M. EpCAM-KO cancer cells (Figure 4e).

EpCAM-ReTARG^{pp65} redirects the cytotoxic activity of anti-CMV_{pp65} $CD8^{pos}$ T cells toward $EpCAM^{pos}$ carcinoma cell lines of diverse origins

The capacity of EpCAM-ReTARG^{pp65} to redirect the cytotoxic activity of *ex vivo*-expanded anti-CMV_{pp65} $CD8^{pos}$ T cells toward $EpCAM^{pos}$ human cancer cell lines was assessed. EpCAM-ReTARG^{pp65} redirected anti-CMV_{pp65} $CD8^{pos}$ T cells toward PC-3 M, OvCAR-3 and NCI-H292 cancer cells in a dose-dependent (Figure 5a) and E:T cell ratio-dependent manner (Figure 5b,c,d). A panel of 10 $EpCAM^{pos}$ and three $EpCAM^{neg}$ cancer cell lines was evaluated. In the presence of EpCAM-ReTARG^{pp65} and anti-CMV_{pp65} $CD8^{pos}$ T cells, all $EpCAM^{pos}$ cancer cell

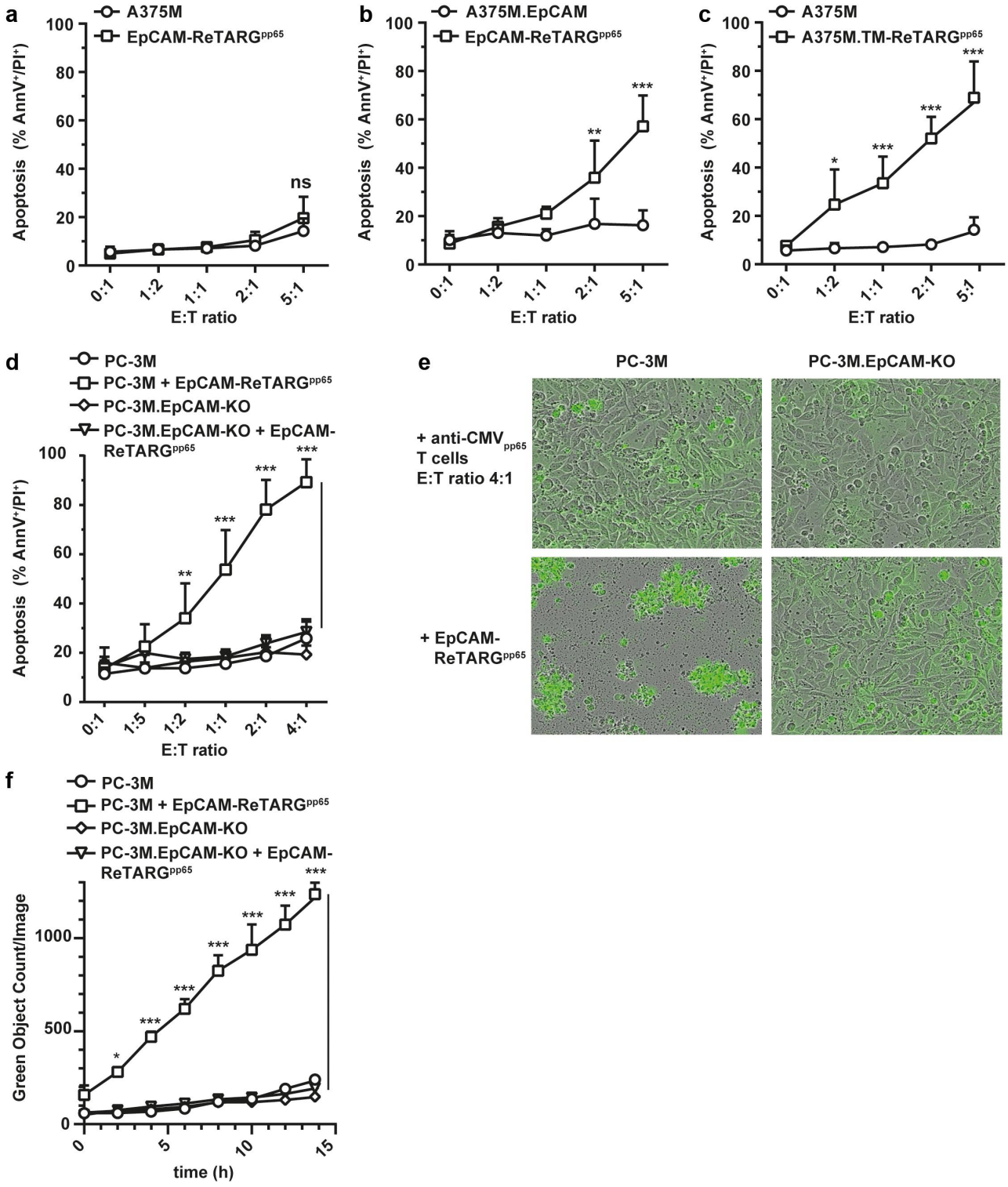

Figure 3. EpCAM-ReTARG^{pp65} engages anti-CMV$_{pp65}$ CD8^{pos} T cells in an EpCAM-selective manner. Cytotoxic capacity of anti-CMV$_{pp65}$ CD8^{pos} T cells toward (a) EpCAM^{neg} A375M, (b) A375 M.EpCAM, and (c) A375M.transmembrane(TM)-ReTARG^{pp65} melanoma cells at increasing E:T cell ratios in the presence (or absence) of EpCAM-ReTARG^{pp65} (100 ng/ml). Apoptotic cancer cell death was assessed using Annexin-V/PI staining after 24 h. A375M.TM-ReTARG^{pp65} cells were used as positive control. (d) Cytotoxic capacity of anti-CMV$_{pp65}$ CD8^{pos} T cells toward PC-3 M and PC-3 M.EpCAM-KO cancer cells at increasing E:T cell ratios in the presence (or absence) of EpCAM-ReTARG^{pp65} (100 ng/ml). Apoptotic cancer cell death was assessed using Annexin-V/PI staining after 24 h. (e,f) Cytotoxic capacity of anti-CMV$_{pp65}$ CD8^{pos} T cells toward PC-3 M and PC-3 M.EpCAM-KO cancer cells (E:T cell ratio = 4:1) in the presence (or absence) of EpCAM-ReTARG^{pp65} (100 ng/ml) using a conditionally fluorescent caspase-3/8 substrate. Representative images shown were taken after 15 h at 10× magnification. Quantification of green fluorescent cells over time is shown. The ex vivo-expanded T cells used were from CMV-seropositive/HLA-B × 07:02^{pos} donor #2. Graphs A-D: $n = 3$ (two technical replicates), mean ± SD are shown. Graph F shows a representative image with two technical replicates (mean ± SD). Statistical analysis in A-C was performed using two-way ANOVA followed by Bonferroni-Dunn post-hoc test. Statistical analysis in D+F was performed using two-way ANOVA followed by Bonferroni-Dunn post-hoc test (PC-3 M + EpCAM-ReTARG^{pp65} vs PC-3 M.EpCAM-KO + EpCAM-ReTARG^{pp65}). (ns = not significant, *p < .05, **p < .01, ***p < .001).

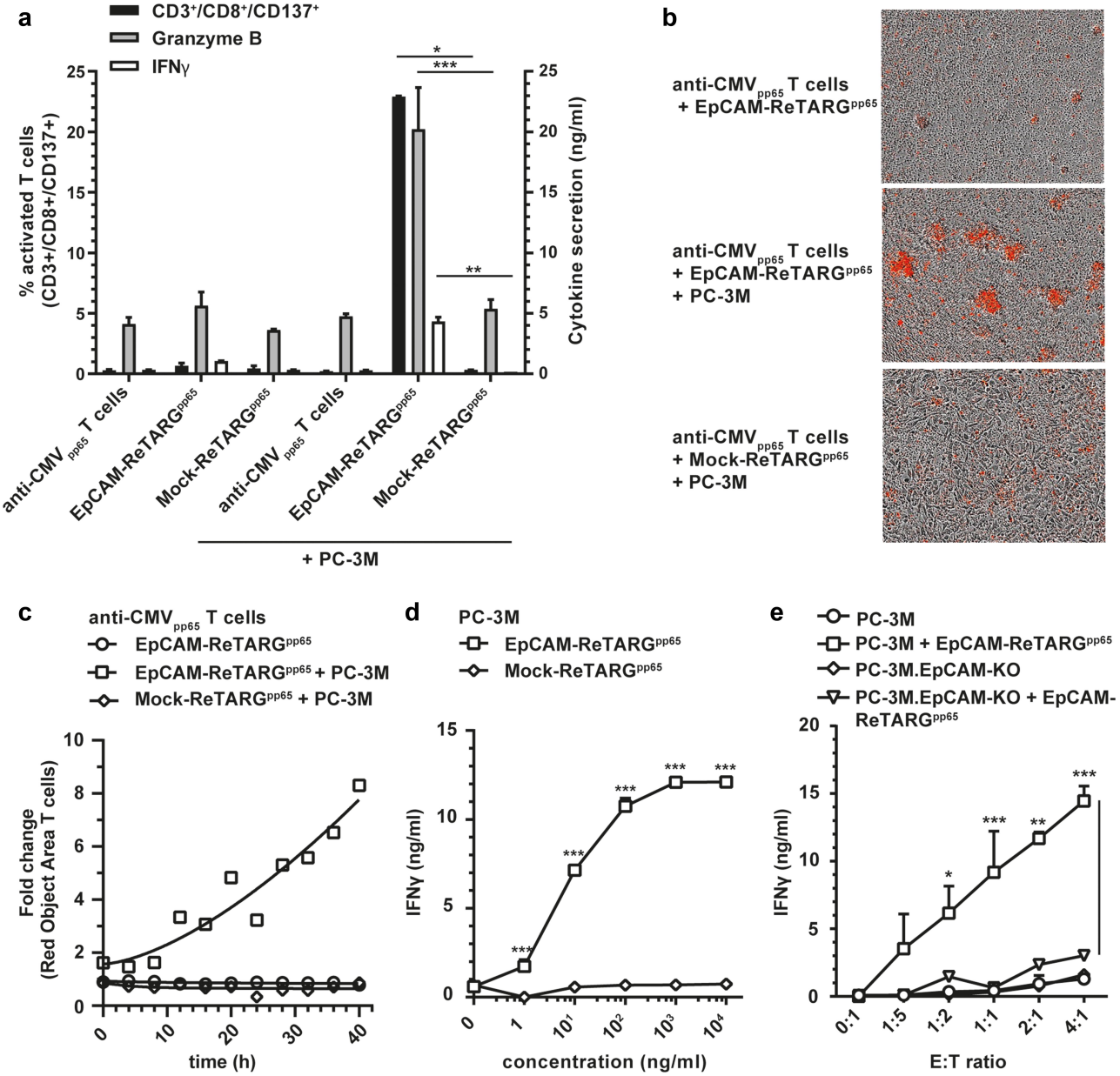

Figure 4. EpCAM-ReTARG^{pp65} selectively activates cytotoxic effector potential of anti-CMV$_{pp65}$ CD8^{pos} T cells. (a) Antigen-specific activation status (CD137 exposure) of anti-CMV$_{pp65}$ CD8^{pos} T cells in presence (or absence) of PC-3 M cancer cells (E:T cell ratio = 2:1), EpCAM-ReTARG^{pp65} and Mock-ReTARG^{pp65} (both 100 ng/ml) after 24 h. Subsequently, conditioned culture media was collected and analyzed for T cell-secreted Granzyme B and IFNγ by appropriate ELISAs. (b,c) Analysis of proliferation and subsequent aggregate formation of CFSE-labeled anti-CMV$_{pp65}$ CD8^{pos} effector T cells cocultured (or not) with PC-3 M target cells (E:T cell ratio = 2:1) in presence of EpCAM-ReTARG^{pp65} and Mock-ReTARG^{pp65} (both 100 ng/ml) by live cell imaging. Representative images shown were taken after 40 h at a 10× magnification. Size of T cell clusters (Red Object Area (μm^2/image)) is shown as fold change over time. (d) Capacity of EpCAM-ReTARG^{pp65} and Mock-ReTARG^{pp65} at increasing concentrations to activate anti-CMV$_{pp65}$ CD8^{pos} T cells in the presence of EpCAM^{pos} PC-3 M cells (E:T cell ratio = 2:1). Conditioned culture media was collected after 24 h and T cell-secreted IFNγ quantified by ELISA. (e) Capacity of EpCAM-ReTARG^{pp65} (100 ng/ml) to activate anti-CMV$_{pp65}$ CD8^{pos} T cells in the presence of EpCAM^{pos} PC-3 M and PC-3 M.EpCAM-KO cancer cells at increasing E:T cell ratios. Conditioned culture media was collected after 24 h and T cell-secreted IFNγ quantified by ELISA. The ex vivo-expanded T cells used were from CMV-seropositive/HLA-B × 07:02^{pos} donor #2. All graphs show representative images with two technical replicates (mean ± SD). Statistical analysis in a was performed using unpaired t-test. Statistical analysis in D was performed using two-way ANOVA followed by Bonferroni-Dunn post-hoc test. Statistical analysis in E was performed using two-way ANOVA followed by Bonferroni-Dunn post-hoc test (PC-3 M + EpCAM-ReTARG^{pp65} vs PC-3 M.EpCAM-KO + EpCAM-ReTARG^{pp65}). (*p < .05, **p < .01, ***p < .001).

lines were eliminated, whereas all EpCAM^{neg} cancer cell lines remained essentially unaffected (Table S1). The intrinsic sensitivity of the cancer cell lines to EpCAM-ReTARG^{pp65} did not appear to depend on differential EpCAM expression. Of note, the EpCAM-selective binding activity and capacity of EpCAM-ReTARG^{pp65} to induce anti-CMV$_{pp65}$ CD8^{pos} T cell-mediated cancer cell elimination were preserved after prolonged storage (3 d) in PBS at various temperatures (Figure S3a,b) and in acetate buffer (pH 4.0 to pH 7.0 (Figure S3c,d)).

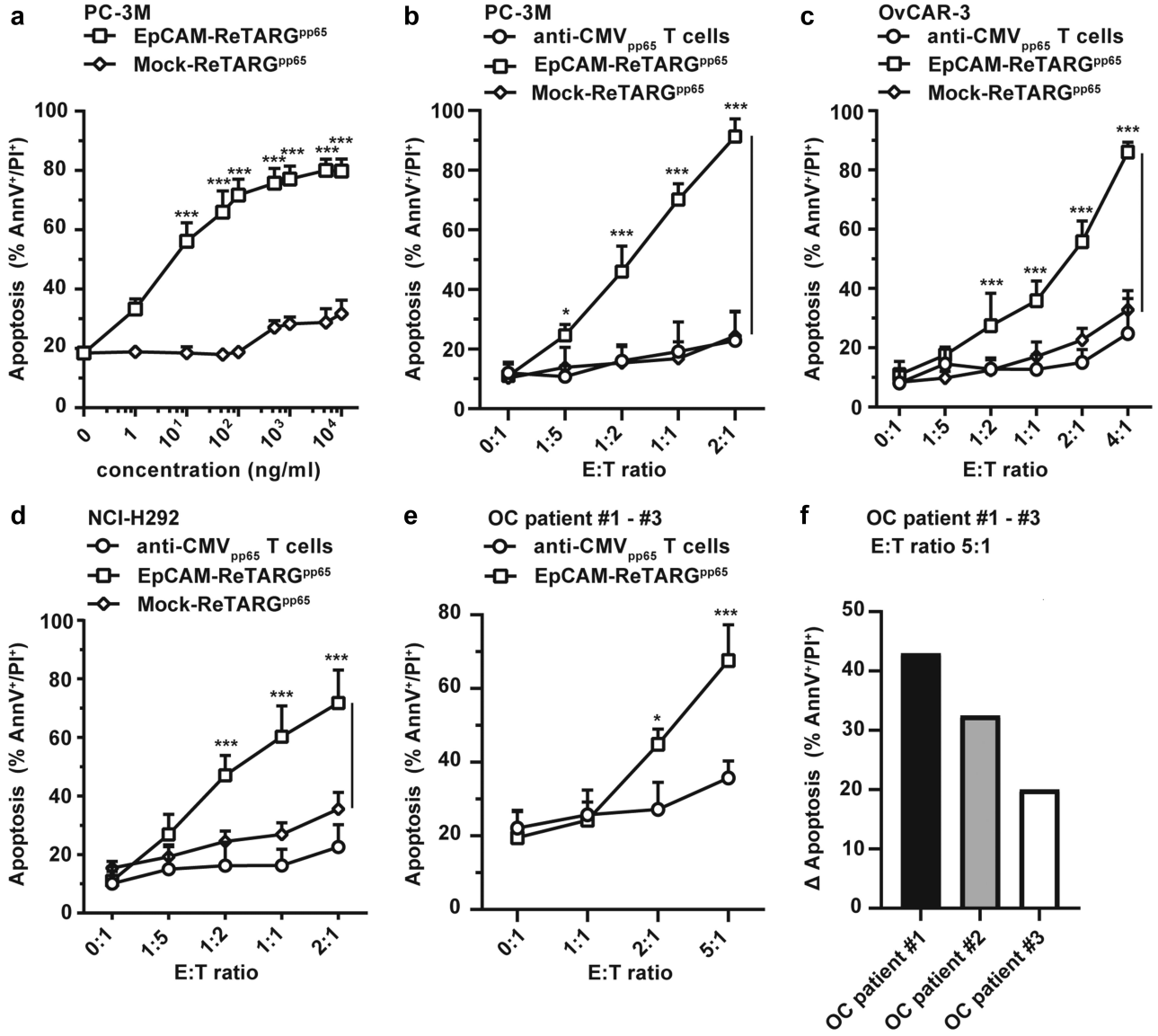

Figure 5. EpCAM-ReTARG^{pp65} redirects the cytotoxic activity of anti-CMV$_{pp65}$ CD8^{pos} T cells toward EpCAM^{pos} carcinoma cell lines of diverse origins and primary patient-derived cancer cells. (a) Cytotoxic capacity of anti-CMV$_{pp65}$ CD8^{pos} T cells toward PC-3 M cancer cells (E:T cell ratio = 2:1) in the presence of increasing concentrations of EpCAM-ReTARG^{pp65} and Mock-ReTARG^{pp65}. Cytotoxic capacity of anti-CMV$_{pp65}$ CD8^{pos} T cells toward (b) PC-3 M; (c) OvCAR-3; (d) NCI-H292 cancer cells at increasing E:T cell ratios in the presence (or absence) of EpCAM-ReTARG^{pp65} and Mock-ReTARG^{pp65} (both 100 ng/ml). (e) Cytotoxic capacity of anti-CMV$_{pp65}$ CD8^{pos} T cells toward cancer samples from 3 patients with stage IIIC high-grade serous ovarian cancer at increasing E:T cell ratios in the presence (or absence) of EpCAM-ReTARG^{pp65} (100 ng/ml). Data obtained from all patient samples were pooled. (f) Cancer cell elimination at E:T cell ratio 5:1 is shown per patient as Δ(+EpCAM-ReTARG^{pp65} - anti-CMV$_{pp65}$ T cells) in %. The ex vivo-expanded T cells used were from CMV-seropositive/HLA-B × 07:02^{pos} donor #2. Graphs A-D: $n = 3$ (two technical replicates), mean ± SD are shown. Graph E shows biological replicates (mean ± SD). Statistical analysis in A-D was performed using two-way ANOVA followed by Bonferroni-Dunn post-hoc test (EpCAM-ReTARG^{pp65} vs Mock-ReTARG^{pp65}). Statistical analysis in E was performed using two-way ANOVA followed by Bonferroni-Dunn post-hoc test. (*p < .05, ***p < .001).

EpCAM-ReTARG^{pp65} redirects the cytotoxic activity of anti-CMV$_{pp65}$ CD8^{pos} T cells toward EpCAM^{pos} primary patient-derived cancer cells

Additionally, the capacity of EpCAM-ReTARG^{pp65} to redirect the cytotoxic activity of *ex vivo*-expanded anti-CMV$_{pp65}$ CD8^{pos} T cells toward EpCAM^{pos} cancer cells from patients with stage IIIC high-grade serous ovarian cancer was evaluated. EpCAM-ReTARG^{pp65} redirected anti-CMV$_{pp65}$ CD8^{pos} T cells to eliminate cancer cells from all three patients (Figure 5e,f).

EpCAM-ReTARG^{pp65} redirects anti-CMV$_{pp65}$ CD8^{pos} T cells to potently eliminate EpCAM^{pos} cancer cells in absence of excessive cytokine release

In vivo, non-physiological overstimulation of T cells by bispecific T-cell engagers (BiTEs) is frequently associated with the induction of massive cytokine release, which can cause severe immune-related side effects. Therefore, we compared the differential cancer cell elimination capacity mediated by EpCAM-ReTARG^{pp65} vs. solitomab and the respective levels of T cell-secreted cytokines.

BiTE solitomab acts by redirecting the cytotoxic activity of all CD3^{pos} T cells toward EpCAM^{pos} cancer cells by activating the CD3ε chain of T cell receptors (TCRs), irrespective of the intrinsic T cell specificity. To allow for an appropriate comparison of EpCAM-ReTARG^{pp65} and solitomab with equal numbers of available effector T cells, the number of *ex vivo*-expanded anti-CMV$_{pp65}$ CD8^{pos} T cells in the presence of solitomab was adjusted to match the percentage of TPR-dextramer^{pos} cells.

Co-culture of effector T cells and PC-3 M target cells with increasing concentrations of EpCAM-ReTARG^{pp65} resulted in an s-shaped dose-response curve with a long exponential phase before reaching maximal cancer cell elimination. For EpCAM-ReTARG^{pp65} the plateau phase was reached at a dose of 500 ng/ml onwards. In contrast, the s-shaped dose-response curve of solitomab was characterized by a markedly shorter exponential phase, reaching maximal cancer cell elimination from a dose of 5 ng/ml onwards (Figure 6a). Half maximal effective concentrations (EC50) are 16.06 ng/ml and 0.53 ng/ml for EpCAM-ReTARG^{pp65} and solitomab, respectively. EpCAM-ReTARG^{pp65} mediates a more gradual elimination of cancer cells, which may allow for more controllable dosing. Increasing concentrations of EpCAM-ReTARG^{pp65} mediated the secretion of IFNγ by T cells to a markedly lesser extent than solitomab did (Figure 6b). The levels of T cell-secreted Granzyme B remained similar for all evaluated concentrations of EpCAM-ReTARG^{pp65}, whereas solitomab enhanced Granzyme B excretion in a dose-dependent manner (Figure 6c). Apparently, ~10 ng/ml of T cell-secreted Granzyme B is sufficient to mediate maximal cancer cell elimination. A dose of 500 ng/ml EpCAM-ReTARG^{pp65} conveyed comparable (maximal) T cell-mediated cancer cell elimination

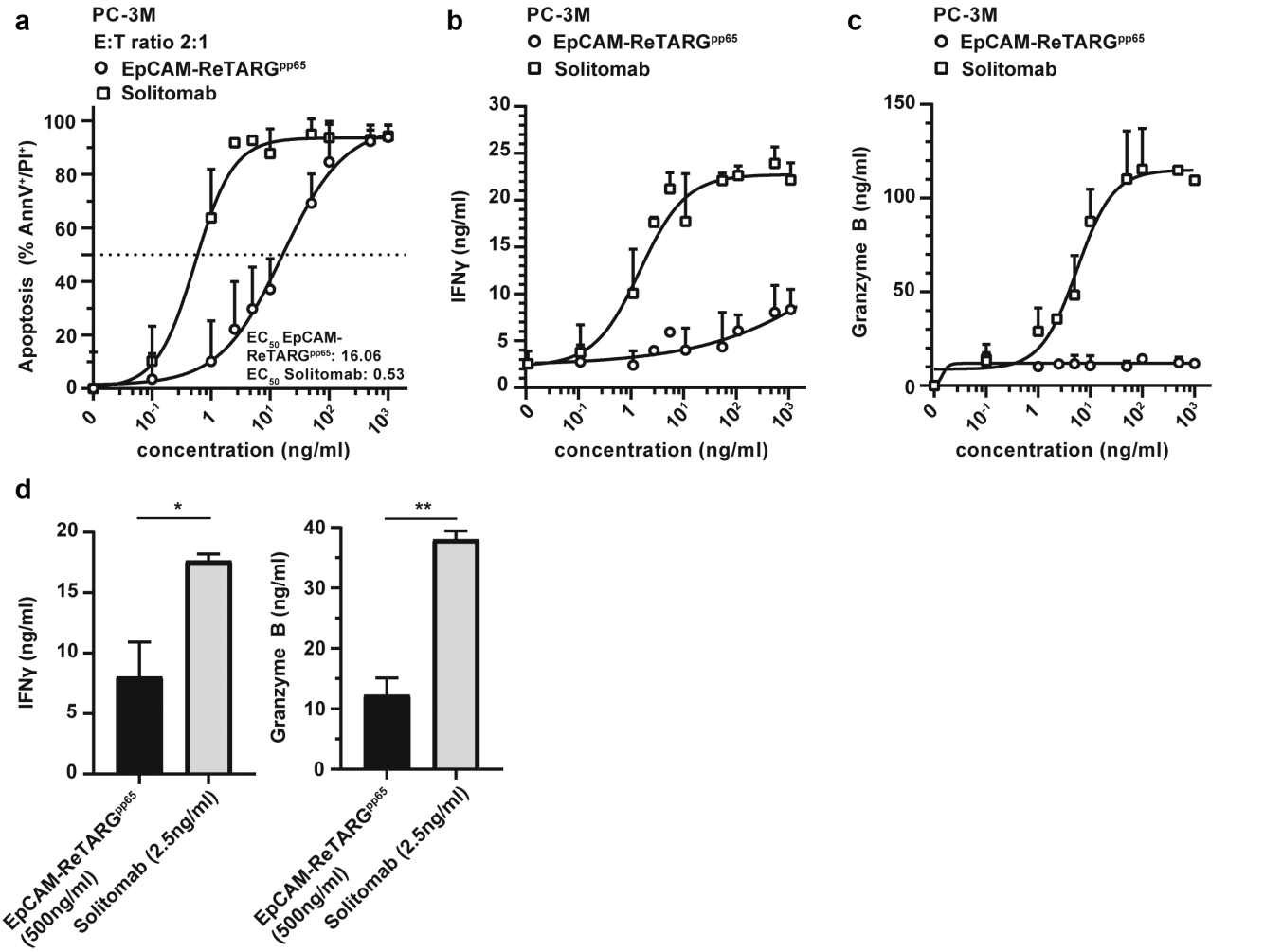

Figure 6. EpCAM-ReTARG^{pp65} redirects anti-CMV$_{pp65}$ CD8^{pos} T cells to potently eliminate cancer cells in absence of excessive cytokine release. (a) Cytotoxic capacity of anti-CMV$_{pp65}$ CD8^{pos} T cells toward EpCAM^{pos} PC-3 M cancer cells (E:T cell ratio = 2:1) in the presence of increasing concentrations of EpCAM-ReTARG^{pp65} and BiTE solitomab. Apoptotic cancer cell death was assessed using Annexin-V/PI staining after 24 h. Background killing was subtracted and maximal cancer cell elimination set to 100%. EC$_{50}$ = half maximal effective concentration. Conditioned cell culture supernatants were collected and analyzed for T cell-secreted (b) IFNγ and (c) Granzyme B by ELISA. (d) Comparison of IFNγ and Granzyme B levels at relevant concentrations of EpCAM-ReTARG^{pp65} and solitomab, which convey comparable (maximal) T cell-mediated cancer cell elimination. Of note, BiTE solitomab acts by redirecting the cytotoxic activity of T cells toward EpCAM^{pos} cancer cells by activating the CD3ε chain of their TCRs, irrespective of their intrinsic specificity. To allow for an appropriate comparison of EpCAM-ReTARG^{pp65} and solitomab with equal numbers of available effector T cells, the amount of ex vivo-expanded anti-CMV$_{pp65}$ CD8^{pos} T cells in the presence of solitomab was adjusted to match the percentage of TPR-dextramer^{pos} cells, which was found to be 50%. The ex vivo-expanded T cells used were from CMV-seropositive/HLA-B × 07:02^{pos} donor #2. Graph A: $n = 3$ (two technical replicates), mean ± SD are shown. Graphs B-D show representative images with two technical replicates (mean ± SD). Statistical analysis in D was performed using unpaired t-test (*p < .05, **p < .01).

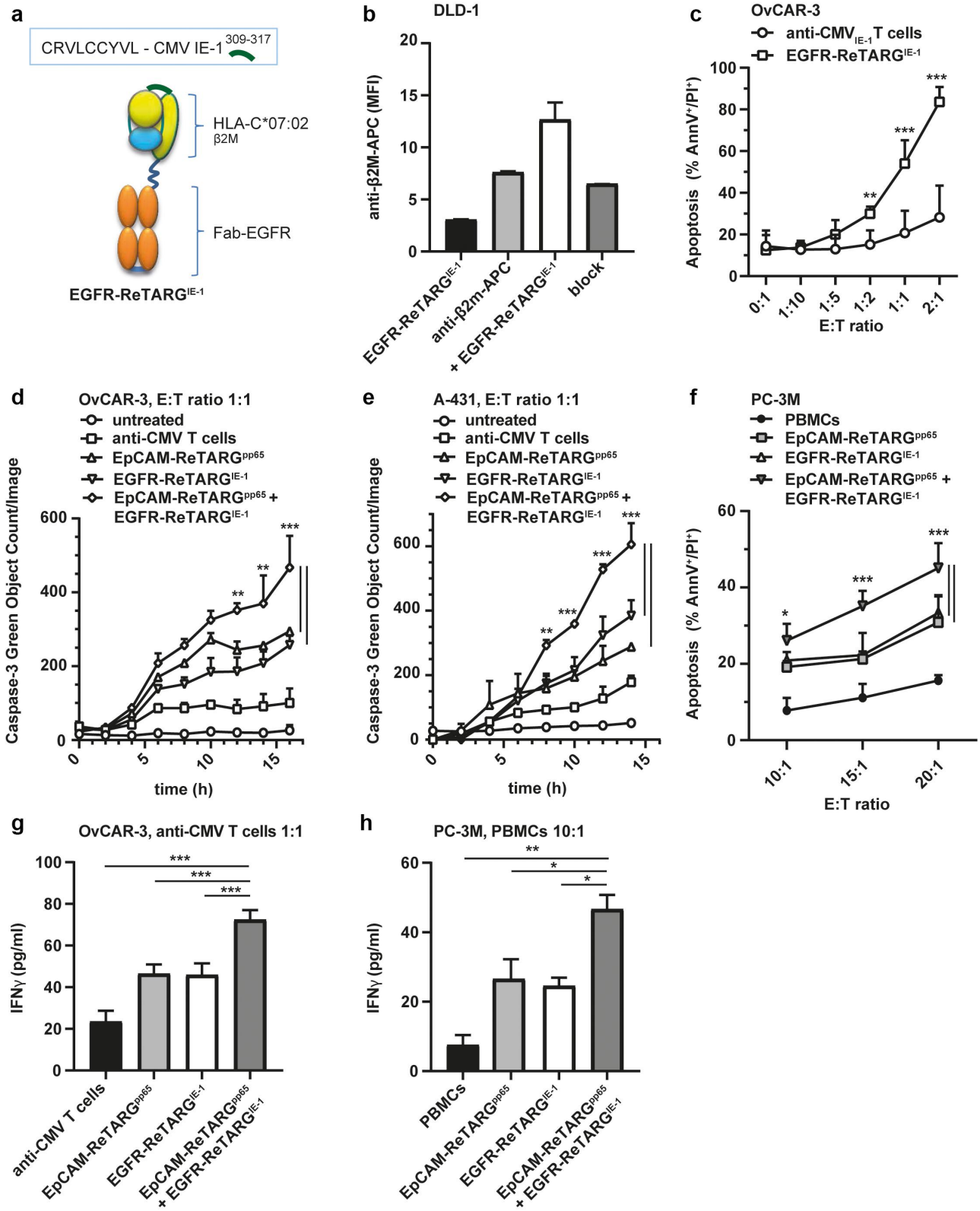

Figure 7. Combinatorial treatment with ReTARG fusion proteins potentiates cancer cell elimination. (a) Schematic representation of EGFR-ReTARG^{IE-1} fusion protein. The anti-EGFR Fab domain of EGFR-ReTARG^{IE-1} was constructed using published VH and VL gene sequences of mAb 425[21]. (b) Binding of EGFR-ReTARG^{IE-1} (0.5 µg/ml) toward EGFR^{pos} DLD-1 cancer cells. Of note, DLD-1 cells are β2 M-deficient. (c) Cytotoxic capacity of anti-CMV$_{IE-1}$ CD8^{pos} T cells toward EGFR^{pos} OvCAR-3 cancer cells at increasing E:T cell ratios in the presence (or absence) of EGFR-ReTARG^{IE-1} (100 ng/ml). Apoptotic cancer cell death was evaluated by Annexin-V/PI staining after 24 h. Cytotoxic capacity of a 1:1 mix of HLA-B × 07:02-restricted anti-CMV$_{pp65}$ CD8^{pos} T cells and HLA-C × 07:02-restricted anti-CMV$_{IE-1}$ CD8^{pos} T cells toward EpCAM^{pos}/EGFR^{pos} (d) OvCAR-3 and (e) A-431 cancer cells (E:T cell ratio = 1:1) in the presence (or absence) of EpCAM-ReTARG^{pp65} or/and EGFR-ReTARG^{IE-1} (both 100 ng/ml) using a conditionally fluorescent caspase-3/8 substrate. Quantification of green fluorescent cells over time is shown. (f) Cytotoxic capacity of freshly isolated PBMCs toward EpCAM^{pos}/EGFR^{pos} PC-3 M cancer cells (E:T cell ratio = 10:1–20:1) in the presence (or absence) of EpCAM-ReTARG^{pp65} or/and EGFR-ReTARG^{IE-1} (both 100 ng/ml). Apoptotic cancer cell death was evaluated by Annexin-V/PI staining after 4 d. (g) Capacity of EpCAM-ReTARG^{pp65} and EGFR-ReTARG^{IE-1} (both 100 ng/ml) to activate a 1:1 mix of anti-CMV$_{pp65}$/anti-CMV$_{IE-1}$ CD8^{pos} T cells in the presence of OvCAR-3 cancer cells (E:T cell ratio = 1:1). Conditioned culture media was collected after 24 h and

T cell-secreted IFNγ was quantified by ELISA. (h) Capacity of EpCAM-ReTARG^{pp65} and EGFR-ReTARG^{IE-1} (both 100 ng/ml) to activate PBMCs in the presence of PC-3 M cancer cells (E:T cell ratio = 10:1). Conditioned culture media was collected after 4 d and T cell-secreted IFNγ was quantified by ELISA. The ex vivo-expanded T cells used were from CMV-seropositive/HLA-B × 07:02^{pos} donor #2. Graphs B, D, E, G and H show representative images with two technical replicates (mean ± SD). Graphs C and F: $n = 3$ (two technical replicates), mean ± SD are shown. Statistical analysis in C was performed using two-way ANOVA followed by Bonferroni-Dunn post-hoc test. Statistical analysis in D-F was performed using two-way ANOVA followed by Bonferroni-Dunn post-hoc test (EpCAM-ReTARG^{pp65} + EGFR-ReTARG^{IE-1} vs EpCAM-ReTARG^{pp65} and EGFR-ReTARG^{IE-1}, respectively). Representatively, only the comparison with lower significance level is shown in the graph. Statistical analysis in G+H was performed using one-way ANOVA followed by Bonferroni-Dunn post-hoc test. (*p < .05, **p < .01, ***p < .001).

as solitomab does at≥2.5 ng/ml. At these doses, the level of T cell-secreted IFNγ remained~55% lower when T cells were directed toward cancer cells with EpCAM-ReTARG^{pp65} instead of solitomab. Likewise, EpCAM-ReTARG^{pp65}-redirected T cells secreted~65% less Granzyme B (Figure 6d).

Combinatorial treatment with ReTARG fusion proteins potentiates cancer cell elimination

We constructed EGFR-ReTARG^{IE-1}, in which the CMV IE-1 peptide CRV, a soluble HLA-C × 07:02/β2 M molecule, and an EGFR-directed Fab domain were fused in tandem (Figure 7a). EGFR-ReTARG^{IE-1} showed EGFR-selective binding activity (Figure 7b) and redirected *ex vivo*-expanded anti-CMV$_{IE-1}$ CD8^{pos} T cells to eliminate EGFR^{pos} OvCAR-3 cancer cells (Figure 7c). EGFR-ReTARG^{IE-1} was used to assess whether combinatorial treatment with two distinct ReTARG fusion proteins could be employed to further potentiate cancer cell elimination. Anti-CMV$_{pp65}$ and anti-CMV$_{IE-1}$ CD8^{pos} T cells only eliminated cancer cells in the presence of EpCAM-ReTARG^{pp65} and EGFR-ReTARG^{IE-1}, respectively, whereas HLA/peptide-unmatched anti-CMV CD8^{pos} T cells did not (Figure S4). Enhanced elimination of OvCAR-3 (Figure 7d) and A-431 (Figure 7e) cancer cells was observed when combining EpCAM-ReTARG^{pp65} and EGFR-ReTARG^{IE-1} in the presence of respective cognate anti-CMV CD8^{pos} T cells. Remarkably, combining EpCAM-ReTARG^{pp65} and EGFR-ReTARG^{IE-1} in the presence of freshly isolated PBMCs also induced up to 45% elimination of PC-3 M cancer cells (Figure 7f). The combined presence of EpCAM-ReTARG^{pp65} and EGFR-ReTARG^{IE-1} resulted in an increase in T cell-secreted IFN-γ by ~20 pg/ml (Figure 7g,H).

Discussion

Here, we report the construction and preclinical evaluation of EpCAM-ReTARG^{pp65}, a novel recombinant fusion protein in which CMV pp65-derived peptide TPR, soluble HLA-B × 07:02/β2 M molecule, and an EpCAM-directed Fab antibody domain are genetically fused in tandem. Our data demonstrate that treatment of cancer cells with EpCAM-ReTARG^{pp65} renders both cell lines and primary patient-derived carcinoma cells highly sensitive to the cytolytic capacity of anti-CMV CD8^{pos} T-cells in an EpCAM-directed manner. Remarkably, cancer cells expressing very low EpCAM levels not or barely detectable by flow cytometry, were potently eliminated by cognate anti-CMV T cells when incubated with EpCAM-ReTARG^{pp65}, whereas identically treated EpCAM-KO cancer cells remained unaffected. This observation is in line with reports demonstrating that the initiation of the cytolytic activity of CD8^{pos} T cells requires cognate interaction with as little as three peptide-MHC complexes per target cancer cell[22].

EpCAM-ReTARG^{pp65} was designed as a monomeric fusion protein to prevent untimely T cell activation due to the cross-linking of cognate TCRs in the absence of EpCAM^{pos} target cells. Indeed, in the absence of EpCAM-expressing cancer cells, anti-CMV CD8^{pos} T-cells incubated with EpCAM-ReTARG^{pp65} were not activated (Figure 4).

Subsequently, we explored whether PBMCs freshly derived from CMV-seropositive healthy volunteers contained sufficient amounts of anti-CMV CD8^{pos} T cells to allow EpCAM-ReTARG^{pp65}-mediated elimination of EpCAM-expressing cancer cells without the need for prior *in vitro* activation/expansion. In this respect, the percentage of TPR-dextramer^{pos} T cells present in the PBMCs of our panel of CMV-seropositive HLA-B × 07:02 healthy volunteers ranged from 0.62 to 3.88%. Indeed, without prior *in vitro* expansion/activation, TPR-dextramer^{pos} T cells showed potent capacity to eliminate EpCAM-ReTARG^{pp65}-decorated OvCAR-3. pp65 cancer cells at an E:T cell ratio of 20:1. Using a standard *in vitro* activation/expansion protocol for 15 days increased the percentage of TPR-dextramer^{pos} T cells to~60%, which in turn allowed efficient elimination of EpCAM-ReTARG^{pp65}-decorated OvCAR-3. pp65 cancer cells at E:T cell ratios as low as 2:1 (Figure 2).

The mode of action of EpCAM-ReTARG^{pp65} involves EpCAM-directed formation of a functional cytolytic immune synapse between a cognate effector T cell and an EpCAM-expressing cancer target cell. We wondered whether the molecular size of EpCAM-ReTARG^{pp65} negatively affects the functionality of the cytolytic immune synapse. Therefore, we compared the capacity of anti-CMV pp65 CD8^{pos} T cells to eliminate HLA-B × 07:02^{pos} cancer cells decorated with EpCAM-ReTARG^{pp65}, cancer cells ectopically expressing a smaller transmembrane version of ReTARG^{pp65} (TM-ReTARG^{pp65}), and cancer cells exogenously loaded with the corresponding pp65-derived TPR peptide. These results indicated that the presence of EpCAM-ReTARG^{pp65} in immune synapse formation does not compromise the full cytolytic potential of the redirected cognate effector T cells.

Recently, it was demonstrated that HLA-C × 07:02-restricted anti-CMV CD8^{pos} T cells directed at the CMV IE-1-derived peptide CRVLCCYVL massively expanded during healthy aging, thereby dominating the memory CD8^{pos} T cell pool (without signs of exhaustion) in people aged>70 years[18]. As cancer is more prevalent in the elderly, we constructed and evaluated the fusion protein EGFR-ReTARG^{IE-1} with the engineered capacity to redirect HLA-C × 07:02-restricted anti-CMV$_{IE-1}$ CD8^{pos}T cells to attack cancer cells in an EGFR-directed manner. Our data demonstrated that treatment of cancer cells with EGFR-ReTARG^{IE-1} renders cancer cell lines

sensitive to the cytolytic capacity of inflationary anti-CMV_{IE-1} $CD8^{pos}$ T cells. Moreover, combinatorial treatment of $EpCAM^{pos}/EGFR^{pos}$ cancer cells with EpCAM-$ReTARG^{pp65}$ and EGFR-$ReTARG^{IE-1}$ strongly potentiated cancer cell elimination compared with single-agent treatment. Haplotypes HLA-B × 07:02 and HLA-C × 07:02 frequently co-occur[23]. Hence, combinatorial treatment with EpCAM-$ReTARG^{pp65}$ and EGFR-$ReTARG^{IE-1}$ appears suitable for a significant patient subset (~20%). It is tentative to speculate that combination treatment with EpCAM-$ReTARG^{pp65}$ and EGFR-$ReTARG^{IE-1}$ may reduce the risk of antigen escape by cancer cells. Additionally, combinatorial treatment with multiple ReTARG fusion proteins may reduce the need for *ex vivo* expansion of anti-CMV $CD8^{pos}$ T cells.

Treatment of cancer cells with BiTEs aims to activate and redirect essentially all the patients' $CD3^{pos}$ T cells toward cancer cells, irrespective of T cell subtype and/or intrinsic TCR specificity. BiTE-based therapies are typically associated with a massive release of proinflammatory cytokines, including IFNγ. High levels of proinflammatory cytokines may result in considerable *in vivo* toxicity, usually manifested as cytokine release syndrome[24]. In our experiments, we titrated EpCAM-$ReTARG^{pp65}$ and BiTE solitomab concentrations to the level at which maximum cancer cell elimination was achieved. A significantly higher dose of EpCAM-$ReTARG^{pp65}$ than that of solitomab was required to achieve maximal killing. However, the concurrent level of T cell-secreted IFNγ induced by EpCAM-$ReTARG^{pp65}$ treatment was~66% lower. In addition, *in vitro* the dose-responsiveness of EpCAM-$ReTARG^{pp65}$ appeared to be much more gradual than that of solitomab. This suggests a potentially better controllability of EpCAM-$ReTARG^{pp65}$ *in vivo* in terms of therapeutic dosing, which may help to mitigate immune-related adverse events. The observed difference in the concentration of EpCAM-$ReTARG^{pp65}$ vs. solitomab required to achieve maximal cancer cell elimination may be related to their rather different molecular natures, modes of action, and possible differences in binding affinities for cancer cell-exposed EpCAM. Moreover, differences in the in-solution behavior and size of these two distinct classes of molecules may influence key pharmacokinetic characteristics, such as *in vivo* half-life and anticancer efficacy. These and other *in vivo* therapeutically relevant aspects of the EpCAM-$ReTARG^{pp65}$ approach require follow-up evaluation in appropriate animal tumor models.

Recently, various strategies have been proposed to selectively redirect anti-CMV T cells toward cancer cells. Millar *et al.* (2020) demonstrated that antibody-peptide epitope conjugates (APECs) deliver CMV-derived peptides to empty HLA-I complexes on the surface of cancer cells. Upon presentation of CMV-derived CTL epitopes into empty HLA-I complexes, the cancer cells were efficiently eliminated. Remarkably, in contrast to BiTEs, APECs did not activate Tregs[25].

Jung *et al.* (2022) developed a $CD8^{pos}$ T cell epitope-delivering antibody (TEDbody) that delivered the CMV pp65 peptide NLV via the tumor-associated receptor integrin αvβ5 to the cytosol of cancer cells. Conforming to the class I antigen-processing pathway, NLV is present on HLA-A × 02:01 on the surface of cancer cells, which elicits their elimination by anti-CMV $CD8^{pos}$ T cells. In an immunodeficient mouse model, TEDbody suppressed tumor growth in the presence of anti-CMV $CD8^{pos}$ T-cells[26].

However, the above-mentioned alternative strategies strictly rely on intact antigen-processing and -presenting pathways and/or (empty) HLA-I surface expression to render cancer cells susceptible to anti-CMV $CD8^{pos}$ T cell lysis. Unfortunately, cancer cells often downregulate HLA-I surface exposure, which prevents recognition by $CD8^{pos}$ T cells[27]. ReTARG fusion proteins were engineered to contain peptide-equipped HLA-I complexes, and thus did not depend on endogenous HLA-I expression. In this respect, the ReTARG approach can be applied despite defects in antigen processing and presentation pathways, which are common in various cancer types.

Besides its tumoricidal activity, it is conceivable that the ReTARG approach may also promote the expansion of cognate anti-CMV T cells present in the tumor microenvironment and contribute to long-term disease control. This attribute of the ReTARG approach may be of relevance to cancer types in which CMV appears to be implicated in tumorigenesis[28].

To evaluate whether patients would be eligible for treatment with ReTARG fusion proteins, CMV infection status and HLA-I haplotypes need to be determined. With a prevalence of approximately 83% in the general population, the requirement of seropositivity does not appear to be a major obstacle for the majority of patients[29]. Moreover, EpCAM-$ReTARG^{pp65}$ and EGFR-$ReTARG^{IE-1}$ are equipped with the highly prevalent haplotypes HLA-B × 07:02 (present in~15–25%) and HLA-C × 07:02 (present in~20–30%), respectively[30]. To include even larger parts of the population, we are in the process of constructing additional ReTARG candidates with other common HLA-I haplotypes.

In this study, we demonstrated that the elimination of ReTARG-decorated cancer cells is attributable to cognate anti-CMV $CD8^{pos}$ T cells. However, the involvement of other immune effector cells with cytolytic activity, such as NK cells cannot be completely ruled out. In particular, CMV infection is known to induce the expansion of so-called adaptive NK cells with memory-like properties and increased cytolytic potential[31]. Whether this type of NK cells contributes to ReTARG-mediated cancer cell elimination remains to be determined.

In conclusion, our data demonstrate that Fab antibody domain-based ReTARGs show a potent capacity to redirect anti-CMV $CD8^{pos}$ T cells to selectively eliminate human carcinoma cells. Moreover, *in vitro* treatment with EpCAM-$ReTARG^{pp65}$ rendered primary patient-derived cancer cells highly susceptible to elimination by anti-CMV T-cells. EpCAM-$ReTARG^{pp65}$ and EGFR-$ReTARG^{IE-1}$ were designed for HLA haplotypes HLA-B × 07:02 and HLA-C × 07:02, respectively, which show dominance, both in number and functionality in the anti-CMV T cell pool. In contrast to the corresponding BiTE, EpCAM-$ReTARG^{pp65}$ promoted the cytotoxic activity of T cells without a massive proinflammatory cytokine response known to be associated with various serious immune-related adverse events. Moreover, we showed that combinatorial treatment with EpCAM-$ReTARG^{pp65}$ and EGFR-$ReTARG^{IE-1}$ simultaneously recruits anti-CMV_{pp65} and anti-CMV_{IE-1} $CD8^{pos}$ T cells, thereby enhancing cancer

cell elimination compared to single-agent treatment. Taken together, the ReTARG fusion protein approach may be valuable as a complementary and/or alternative next-generation approach in cancer immunotherapy.

Disclosure statement

No potential conflict of interest was reported by the authors.

Funding

This work was supported by Dutch Cancer Society project numbers 13077 (to W.H.) and GSMS-123015 (to I. B.).

ORCID

Isabel Britsch http://orcid.org/0000-0003-4772-9889
Anne P. van Wijngaarden http://orcid.org/0000-0002-8221-1180
Xiurong Ke http://orcid.org/0000-0001-8982-0950
Mark. A.J.M. Hendriks http://orcid.org/0000-0001-7276-4622
Douwe F. Samplonius http://orcid.org/0000-0002-0613-7150
Emily M. Ploeg http://orcid.org/0000-0002-0735-2020
Wijnand Helfrich http://orcid.org/0000-0001-7004-3995

Data availability statement

All data relevant to the study are included in the article or are uploaded as supplementary information.

References

1. Jenkins RW, Barbie DA, Flaherty KT. Mechanisms of resistance to immune checkpoint inhibitors. Br J Cancer. 2018;118:9–16. doi:10.1038/bjc.2017.434.
2. Syn NL, Teng MWL, Mok TSK, Soo RA. De-novo and acquired resistance to immune checkpoint targeting. Lancet Oncol. 2017;18:e731–741. doi:10.1016/S1470-2045(17)30607-1.
3. O'Donnell JS, L Teng MW, Smyth MJ. Cancer immunoediting and resistance to T cell-based immunotherapy. Nat Rev Clin Oncol. 2019;16:151–167. doi:10.1038/s41571-018-0142-8.
4. O'Hara GA, Welten SPM, Klenerman P, Arens R. Memory T cell inflation: understanding cause and effect. Trends Immunol. 2012;33:84–90. doi:10.1016/j.it.2011.11.005.
5. Khan N, Shariff N, Cobbold M, Bruton R, Ainsworth JA, Sinclair AJ, Nayak L, Moss PA, et al. Cytomegalovirus seropositivity drives the CD8 T Cell repertoire toward greater clonality in healthy elderly individuals. J Immunol. 2002;169:1984–1992. doi:10.4049/jimmunol.169.4.1984.
6. Ouyang Q, Wagner WM, Wikby A, Walter S, Aubert G, Dodi AI, Travers P, Pawelec G. Large numbers of dysfunctional CD8 + T lymphocytes bearing receptors for a single dominant CMV epitope in the very old. J Clin Immunol. 2003;23:247–257. doi:10.1023/A:1024580531705.
7. Wills MR, Carmichael AJ, Mynard K, Jin X, Weekes MP, Plachter B, Sissons JG. The human cytotoxic T-lymphocyte (CTL) response to cytomegalovirus is dominated by structural protein pp65: frequency, specificity, and T-cell receptor usage of pp65-specific CTL. J Virol. 1996;70:7569–7579. doi:10.1128/jvi.70.11.7569-7579.1996.
8. Snyder CM, Cho KS, Bonnett EL, van Dommelen S, Shellam GR, Hill AB. Memory inflation during chronic viral infection is maintained by continuous production of short-lived, functional T cells. Immunity. 2008;29:650–659. doi:10.1016/j.immuni.2008.07.017.
9. Derhovanessian E, Maier AB, Hähnel K, Beck R, de Craen AJM, Slagboom EP, Westendorp RGJ, Pawelec G. Infection with cytomegalovirus but not herpes simplex virus induces the accumulation of late-differentiated CD4 + and CD8 + T-cells in humans. J Gen Virol. 2011;92:2746–2756. doi:10.1099/vir.0.036004-0.
10. Wills MR, Okecha G, Weekes MP, Gandhi MK, Sissons PJG, Carmichael AJ. Identification of naive or antigen-experienced human CD8(+) T cells by expression of costimulation and chemokine receptors: analysis of the human cytomegalovirus-specific CD8(+) T cell response. J Immunol. 2002;168:5455–5464. doi:10.4049/jimmunol.168.11.5455.
11. Rosato PC, Wijeyesinghe S, Stolley JM, Nelson CE, Davis RL, Manlove LS, Pennell CA, Blazar BR, Chen CC, Geller MA, et al. Virus-specific memory T cells populate tumors and can be repurposed for tumor immunotherapy. Nat Commun. 2019;10. doi:10.1038/s41467-019-08534-1.
12. Simoni Y, Becht E, Fehlings M, Loh CY, Koo S-L, Teng KWW, Yeong JPS, Nahar R, Zhang T, Kared H, et al. Bystander CD8 + T cells are abundant and phenotypically distinct in human tumour infiltrates. Nature. 2018;557:575–579. doi:10.1038/s41586-018-0130-2.
13. Schmittnaegel M, Levitsky V, Hoffmann E, Georges G, Mundigl O, Klein C, Knoetgen H. Committing cytomegalovirus-specific cd8 t cells to eliminate tumor cells by bifunctional major histocompatibility class i antibody fusion molecules. Cancer Immunol Res. 2015;3:764–776. doi:10.1158/2326-6066.CIR-15-0037.
14. Schmittnaegel M, Hoffmann E, Imhof-Jung S, Fischer C, Drabner G, Georges G, Klein C, Knoetgen H. A new class of bifunctional major histocompatibility class I antibody fusion molecules to redirect CD8 T cells. Mol Cancer Ther. 2016;15:2130–2142. doi:10.1158/1535-7163.MCT-16-0207.
15. Lacey SF, Villacres MC, La Rosa C, Wang Z, Longmate J, Martinez J, Brewer JC, Mekhoubad S, Maas R, Leedom JM, et al. Relative dominance of HLA-B*07 restricted CD8+ T-lymphocyte immune responses to human cytomegalovirus pp65 in persons sharing HLA-A*02 and HLA-B*07 Alleles. Hum Immunol. 2003;64:440–452. doi:10.1016/S0198-8859(03)00028-4.
16. Gillespie GMA, Wills MR, Appay V, O'Callaghan C, Murphy M, Smith N, Sissons P, Rowland-Jones S, Bell JI, Moss PAH. Functional heterogeneity and high frequencies of cytomegalovirus-specific CD8+ T lymphocytes in healthy seropositive donors. J Virol. 2000;74:8140–8150. doi:10.1128/JVI.74.17.8140-8150.2000.
17. Went PT, Lugli A, Meier S, Bundi M, Mirlacher M, Sauter G, Dirnhofer S. Frequent EpCam protein expression in human carcinomas. Hum Pathol. 2004;35:122–128. doi:10.1016/j.humpath.2003.08.026.
18. Hosie L, Pachnio A, Zuo J, Pearce H, Riddell S, Moss P. Cytomegalovirus-specific t cells restricted by HLA-Cw*0702 increase markedly with age and dominate the CD8+ T-Cell repertoire in older people. Front Immunol. 2017;8. doi:10.3389/fimmu.2017.01776.
19. Yang J, Isaji T, Zhang G, Qi F, Duan C, Fukuda T, Gu J. EpCAM associates with integrin and regulates cell adhesion in cancer cells. Biochem Biophys Res Commun. 2020;522:903–909. doi:10.1016/j.bbrc.2019.11.152.
20. Willuda J, Honegger A, Waibel R, Schubiger PA, Stahel R, Zangemeister-Wittke U, Plückthun A. High thermal stability is essential for tumor targeting of antibody fragments: engineering of a humanized anti-epithelial glycoprotein-2 (epithelial cell adhesion molecule) single-chain Fv fragment. Cancer Res. 1999;59:5758–5767.
21. Kettleborough CA, Saldanha J, Heath VJ, Morrison CJ, Bendig MM. Humanization of a mouse monoclonal antibody by CDR-grafting: the importance of framework residues on loop conformation. Protein Eng. 1991;4:773–783. doi:10.1093/protein/4.7.773.
22. Purbhoo MA, Irvine DJ, Huppa JB, Davis MM. T cell killing does not require the formation of a stable mature immunological synapse. Nat Immunol. 2004;5:524–530. doi:10.1038/ni1058.
23. Goldman JL, Miller JO, Miller N, Eveleigh R, Gibson A, Phillips EJ, Pastinen T. HLA-B*07: 02 and HLA-C*07: 02 are associated with trimethoprim-sulfamethoxazole respiratory

failure. Pharmacogenomics J. 2022;22:124–129. doi:10.1038/s41397-022-00266-8.
24. Shimabukuro-Vornhagen A, Gödel P, Subklewe M, Stemmler HJ, Schlößer HA, Schlaak M, Kochanek M, Böll B, von Bergwelt-Baildon MS. Cytokine release syndrome. J ImmunoTher Cancer. 2018;6. doi:10.1186/s40425-018-0343-9.
25. Millar DG, Ramjiawan RR, Kawaguchi K, Gupta N, Chen J, Zhang S, Nojiri T, Ho WW, Aoki S, Jung K, et al. Antibody-mediated delivery of viral epitopes to tumors harnesses CMV-specific T cells for cancer therapy. Nat Biotechnol. 2020;38:420–425. doi:10.1038/s41587-019-0404-8.
26. Jung K, Son M-J, Lee S-Y, Kim J-A, Ko D-H, Yoo S, Kim C-H, Kim Y-S. Antibody-mediated delivery of a viral MHC-I epitope into the cytosol of target tumor cells repurposes virus-specific CD8 + T cells for cancer immunotherapy. Mol Cancer. 2022;21:102. doi:10.1186/s12943-022-01574-0.
27. Aptsiauri N, Carretero R, Garcia-Lora A, Real LM, Cabrera T, Garrido F. Regressing and progressing metastatic lesions: resistance to immunotherapy is predetermined by irreversible HLA class I antigen alterations. Cancer Immunol, Immunother. 2008;57:1727–1733. doi:10.1007/s00262-008-0532-3.
28. Söderberg-Nauclér C. New mechanistic insights of the pathogenicity of high-risk cytomegalovirus (CMV) strains derived from breast cancer: hope for new cancer therapy options. EBioMedicine. 2022;81:104103. doi:10.1016/j.ebiom.2022.104103.
29. Zuhair M, Smit GSA, Wallis G, Jabbar F, Smith C, Devleesschauwer B, Griffiths P. Estimation of the worldwide seroprevalence of cytomegalovirus: a systematic review and meta-analysis. Rev Med Virol. 2019;29:e2034. doi:10.1002/rmv.2034.
30. Gonzalez-Galarza FF, McCabe A, Melo dos Santos EJ, Jones AR, Middleton D. A snapshot of human leukocyte antigen (hla) diversity using data from the Allele Frequency Net Database. Hum Immunol. 2021;82:496–504. doi:10.1016/j.humimm.2020.10.004.
31. Barnes S, Schilizzi O, Audsley KM, Newnes HV, Foley B. Deciphering the immunological phenomenon of adaptive natural killer (NK) cells and cytomegalovirus (CMV). Int J Mol Sci. 2020;21:1–17. doi:10.3390/ijms21228864.